Stem Cell Reports
Article

ISSCR

OPEN ACCESS

WTAP Function in Sertoli Cells Is Essential for Sustaining the Spermatogonial Stem Cell Niche

Gong-Xue Jia,[1,5,6] Zhen Lin,[2,3,6] Rong-Ge Yan,[1,3,6] Guo-Wen Wang,[1,3] Xiao-Na Zhang,[1,3] Cen Li,[4] Ming-Han Tong,[2] and Qi-En Yang[1,3,5,*]

[1]Key Laboratory of Adaptation and Evolution of Plateau Biota, Northwest Institute of Plateau Biology, Chinese Academy of Sciences, Xining, Qinghai, China
[2]State Key Laboratory of Molecular Biology, Shanghai Key Laboratory of Molecular Andrology, CAS Center for Excellence in Molecular Cell Science, Shanghai Institute of Biochemistry and Cell Biology, Chinese Academy of Sciences, Shanghai, China
[3]University of Chinese Academy of Sciences, Beijing, China
[4]Qinghai Provincial Key Laboratory of Tibetan Pharmacology and Safety Evaluation, Northwest Institute of Plateau Biology, Chinese Academy of Sciences, Xining, Qinghai, China
[5]Qinghai Provincial Key Laboratory of Animal Ecological Genomics, Northwest Institute of Plateau Biology, Chinese Academy of Sciences, Xining, Qinghai, China
[6]These authors contributed equally
*Correspondence: yangqien@nwipb.cas.cn
https://doi.org/10.1016/j.stemcr.2020.09.001

SUMMARY

Sertoli cells are the major component of the spermatogonial stem cell (SSC) niche; however, regulatory mechanisms in Sertoli cells that dictate SSC fate decisions remain largely unknown. Here we revealed features of the N^6-methyladenosine (m^6A) mRNA modification in Sertoli cells and demonstrated the functions of WTAP, the key subunit of the m^6A methyltransferase complex in spermatogenesis. m^6A-sequencing analysis identified 21,909 m^6A sites from 15,365 putative m^6A-enriched transcripts within 6,122 genes, including many Sertoli cell-specific genes. Conditional deletion of *Wtap* in Sertoli cells resulted in sterility and the progressive loss of the SSC population. RNA sequencing and ribosome nascent-chain complex-bound mRNA sequencing analyses suggested that alternative splicing events of transcripts encoding SSC niche factors were sharply altered and translation of these transcripts were severely dysregulated by *Wtap* deletion. Collectively, this study uncovers a novel regulatory mechanism of the SSC niche and provide insights into molecular interactions between stem cells and their cognate niches in mammals.

INTRODUCTION

Adult stem cells provide foundation for the homeostasis, growth, and regeneration of most tissues in mammals. Stem cells rely on extrinsic signals from their specialized niches to balance self-renewal and lineage commitment (Jones and Wagers, 2008). The interactions between stem cells and niches also influence stem cell behaviors in aging and pathological conditions (Lukjanenko et al., 2016; Mesa et al., 2015). Identification and functional characterization of niche components and regulatory mechanisms are essential for elucidating the molecular basis of stem cell fate decisions.

Spermatogenesis is a classic stem cell-supported process that requires the activities of spermatogonial stem cells (SSCs). SSCs self-renew to maintain an undifferentiated state and differentiate to produce transient amplifying progenitors that are committed to enter meiosis after several rounds of mitotic divisions (De Rooij, 1988; Oatley and Brinster, 2008). Extrinsic cues from the SSC niche work in concert with intrinsic programs to dictate SSC proliferation, differentiation, and apoptosis (De Rooij, 2017). Sertoli cells serve as the major cellular component of the SSC niche by providing growth factors, extracellular matrix, and structural support (Griswold, 1998; Meng et al., 2000). Sertoli cells also regulate spermatogonial differentiation, meiosis progression, and spermatid development (Griswold, 2018). These specified functions of Sertoli cells are directed by precise gene expression regulation at the transcriptional, post-transcriptional, and translational levels; however, limited knowledge exists about how these regulations are conducted. Elucidating gene regulation programs mediating Sertoli cell-SSC interaction will enhance our understanding of stem cell niche formation and maintenance.

N^6-methyladenosine (m^6A), one of the most widespread modifications in eukaryotic mRNA, has been linked to mRNA stability, structure, splicing, processing, and translational efficiency (TE) (Gilbert et al., 2016; Zhao et al., 2017). The m^6A modification is catalyzed by a multiprotein methyltransferase complex composed of methyltransferase-like 3 (METTL3), METTL14, and Wilms tumor 1-associated protein (WTAP) (Liu et al., 2014). METTL3 functions as the major catalytic subunit, while METTL14 forms a stable heterodimer with METTL3 to enhance methyltransferase activity (Wang et al., 2016). WTAP recruits METTL3 and METTL14 to mRNA targets (Ping et al., 2014). Findings from knockout mouse models uncovered pivotal roles of METTL3- and METTL14-mediated RNA methylation in embryogenesis (Horiuchi et al., 2006), neurogenesis (Wang et al., 2018), and adipogenesis (Kobayashi et al., 2018). In stem cell-dependent tissues, m^6A modification

has critical functions in controlling lineage specification and fate choice of stem and progenitor cells. METTL3-deficient hematopoietic stem cells fail to differentiate properly (Cheng et al., 2019) and *Mettl14* deletion in neural progenitors causes defects in cell cycle progression (Yoon et al., 2017). Moreover, conditional deletion of *Mettl3* or *Mettl14* in germ cells using *Ddx4-Cre* leads to SSC depletion and male sterility (Lin et al., 2017). Despite these key findings, the roles of m^{6}A modification in Sertoli cells are unknown and the functions of WTAP in establishing and maintaining the SSC niche remain to be determined.

Here, using spermatogenesis as a model system, we investigated features and functions of m^{6}A modification in controlling the establishment and maintenance of stem cell niche. We illustrated the m^{6}A methylome and examined the function of WTAP-dependent m^{6}A in Sertoli cells. We showed that WTAP is essential for SSC maintenance and spermatogonial differentiation. Mechanistically, WTAP-mediated m^{6}A modification controlled transcription and translation of a list of genes in Sertoli cells to sustain SSC niche and govern normal spermatogenesis.

RESULTS

WTAP Is Highly Expressed in Murine Sertoli Cells

We firstly examined the expression of m^{6}A methyltransferases WTAP, METTL3, and METTL14 in mouse testis. Immunofluorescent staining revealed that METTL3 or METTL14 was co-localized with WTAP in germ cells and Sertoli cells within seminiferous tubules (Figure S1A). Interestingly, we noticed that immunoreactive signal for WTAP appeared to be strong in Sertoli cells. Co-staining of WTAP, METTL3, or METTL14 with Sertoli cell markers showed that all these proteins were expressed in Sertoli cells and WTAP indeed was strongly enriched in Sertoli cells (Figure 1A). We then examined relative abundances of *Wtap*, *Mettl3*, and *Mettl14* in fluorescence-activated cell sorting isolated Sertoli cells from *Sox9*^{Gfp} transgenic mice. *Wtap* and *Mettl3* transcript concentrations were increased by 5.23-fold and 3.47-fold in SOX9-GFP$^+$ cells compared with those in Sertoli cell-depleted testicular cells (Figure S1B). Together, these data indicated that all three methyltransferases co-existed and likely catalyzed m^{6}A modification in Sertoli cells.

Analysis Features of m^{6}A Modification in Sertoli Cells

As expected, m^{6}A signal was present in Sertoli cells (Figure 2A). To characterize features of m^{6}A, we conducted affinity purification and m^{6}A sequencing in isolated Sertoli cells from adult testis. A total of 21,909 m^{6}A sites were identified from 15,365 putative m^{6}A-enriched transcripts within 6,122 genes (Table S1), and these m^{6}A sites were predominantly distributed in CDS (coding sequence) regions and less abundantly in 3′ UTR and 5′ UTR regions (Figures 1B and S1C). Two-hundred and seventy-eight of 369 previously identified Sertoli cell-specific transcripts (Green et al., 2018) contained m^{6}A sites, such as *Inhbb*, *Wt1*, *Arid4a*, and *Arid4b* (Table S2). *Etv5*, *Ar*, *Dmrt1*, and *Sin3a* transcripts and other genes known to be essential for Sertoli cell function were also included in the m^{6}A-enriched gene list (Figure 1C).

To further decipher potential functions of m^{6}A-enriched transcripts in Sertoli cells, we conducted molecular function classification, phenotype correlation analysis, and gene ontology (GO) analysis (Table S3). The results showed that these transcripts were preferentially associated with nucleic acid binding, hydrolase, enzyme modulator, transcription factor, transferase, and cytoskeleton (Figure 1E). Identified m^{6}A-enriched transcripts were highly relevant to embryonic lethality, abnormal cell physiology, male infertility, abnormal spermatogenesis, and sperm abnormality (Figure 1F). GO analysis of biological process found that these transcripts were enriched in cell proliferation, DNA repair, mRNA export, 3′ end processing, mRNA stability regulation, regulation of translation, and transcription elongation (Figure 1G). In the top 100 of m^{6}A-enriched genes (transcripts with fold enrichment $\geq$24.9), we found genes that have been reported to be essential for spermatogenesis, including *Spaca1* (Fujihara et al., 2012), *Rhox8* (Welborn et al., 2015), and *H3f3b* (Yuen et al., 2014), (Figure S1D). Interestingly, we noticed that a significant number of m^{6}A-enriched transcripts were involved in SSC maintenance and spermatogonial proliferation. For example, *Cxcl12*, *Bmp4*, *Fgf2*, and *Vegfa* transcripts encoding SSC niche factors contained m^{6}A sites (Figure 1D).

Sertoli Cell-Specific Deletion of *Wtap* Caused Male Infertility

Next, we hypothesized that m^{6}A modification in Sertoli cells plays a functional role in regulating SSC niche. To test this hypothesis, we conditionally deleted the *Wtap* by crossing *Wtap*-floxed (*Wtap*$^{fl/fl}$) and *Amh-Cre* mice (Figures S2A and S2B). Immunostaining confirmed a reduction of m^{6}A and WTAP in Sertoli cells of *Wtap*$^{fl/fl}$*Amh-Cre* (hereafter referred to as *Wtap*-sKO) mice (Figure 2A). Testis/body weight ratio of *Wtap*-sKO mice was significantly reduced compared with that of the littermate controls (Figures 2B and 2C). Fertility test showed that *Wtap*-sKO mice were completely sterile (Figure 2D). Caudal epididymal sperm concentration in *Wtap*-sKO mice was only 20.20% of that in control mice (Figures 2E and S2C). H&E staining did not reveal obvious defects in sperm morphology of *Wtap*-sKO mice, and co-staining of the acrosome marker peanut agglutinin (PNA) with mitochondria marker mito-tracker showed that sperm of *Wtap*-sKO animals displayed normal heads and tails (Figures S2D and S2E). PNA staining of

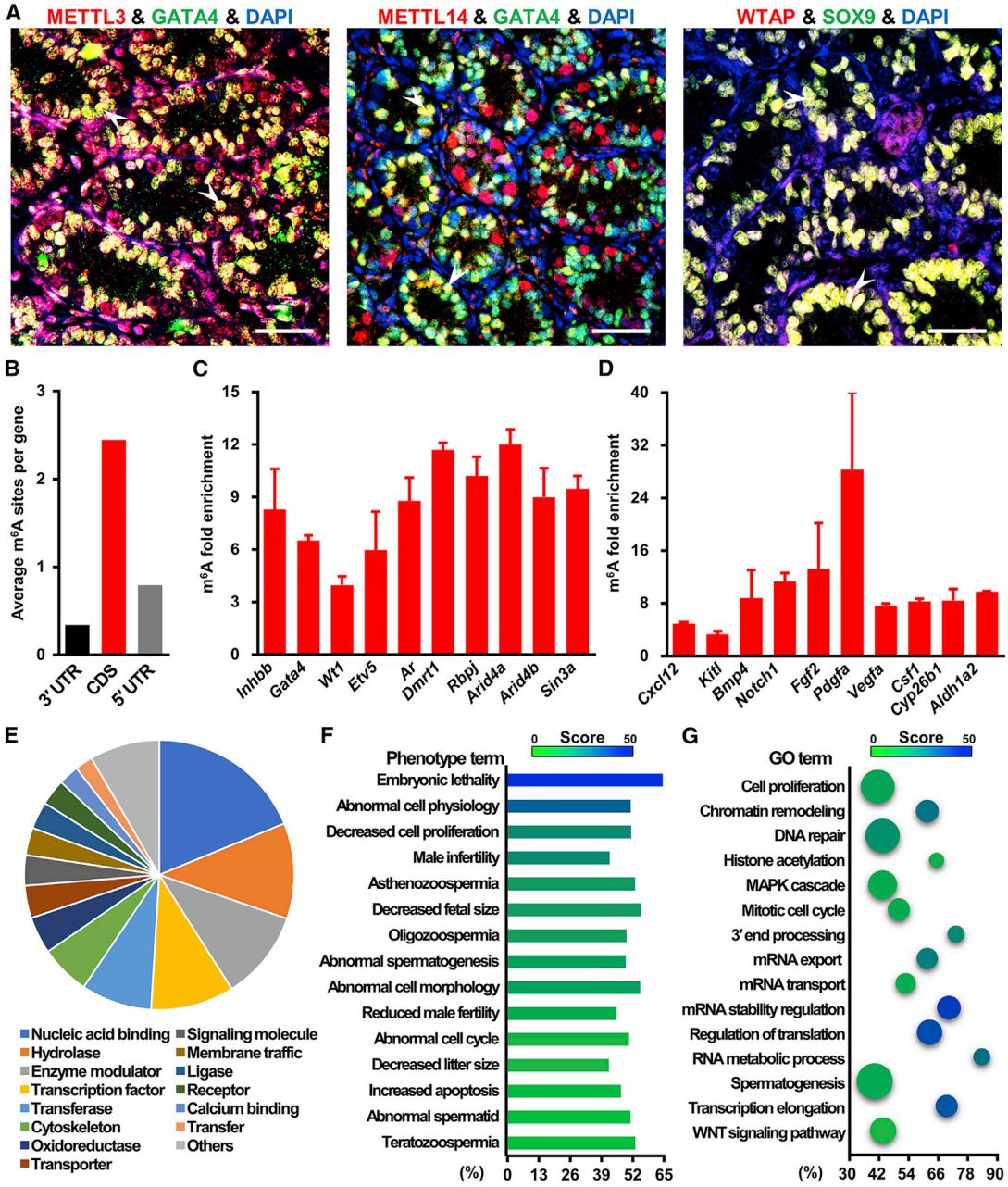

Figure 1. Function Analysis of m^{6}A in Mouse Sertoli Cells

(A) Immunostaining for METTL3 and GATA4, METTL14 and GATA4, or WTAP and SOX9 with DAPI in mouse testes at P6. The arrows indicate Sertoli cells. Scale bars represent 40 μm.

(B) Average m^{6}A sites per gene in distinct RNA sequence regions including 3′ UTR, CDS, and 5′ UTR.

(C and D) Average fold enrichment over input for m^{6}A peaks of selected genes specially expressed in Sertoli cells (C) or related to spermatogenesis (D). Two independent Sertoli cell samples isolated from 110 mice were used (n = 2).

(E–G) Pie chart of molecular types (E), phenotype association analysis (F), and biological process GO analysis (G) of m^{6}A-enriched genes in Sertoli cells. The bubble size indicates the number of matched genes.

See also Figure S1, Tables S1, S2, and S3.

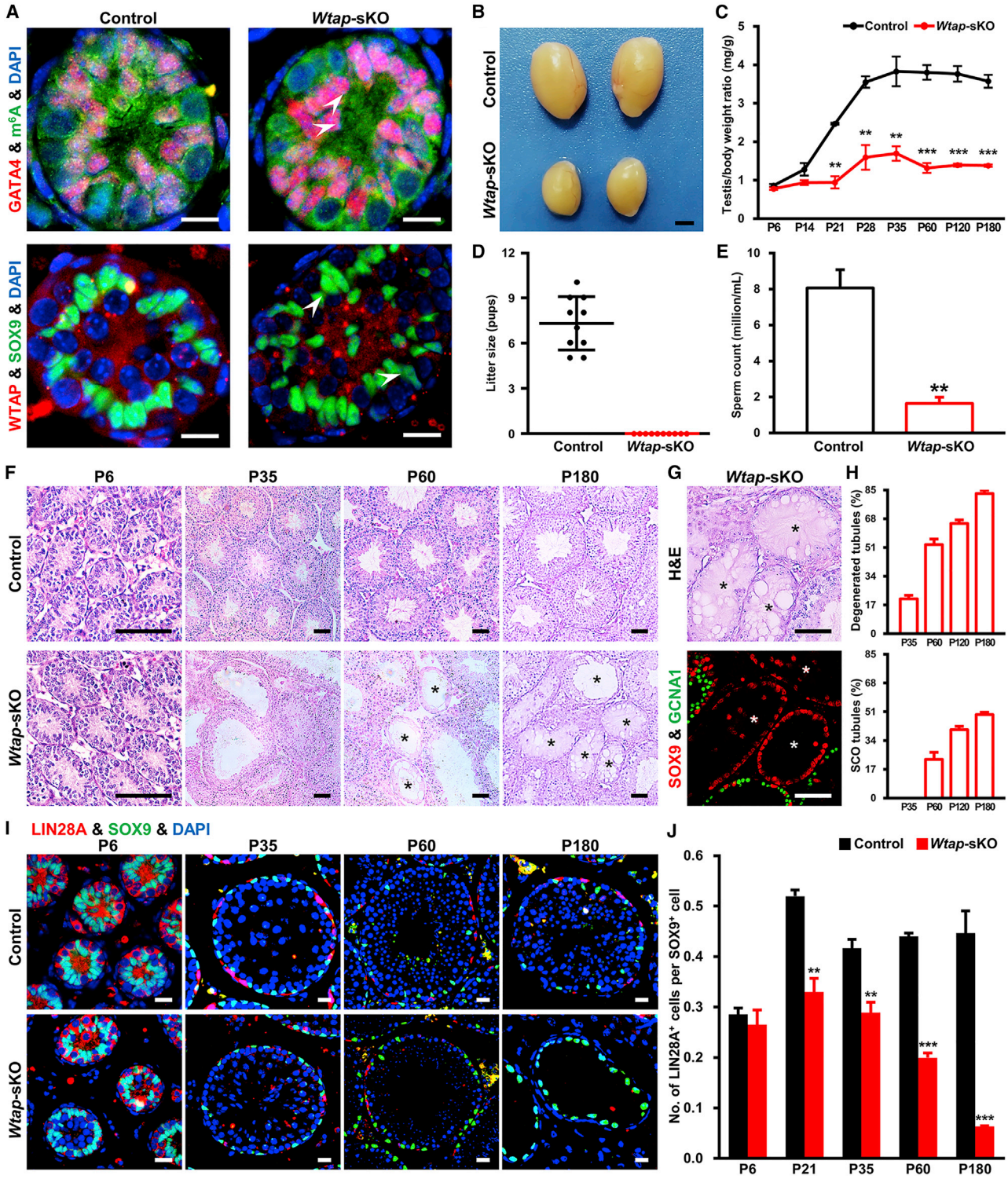

Figure 2. Progressive Loss of Undifferentiated Spermatogonia Caused by *Wtap* Deletion in Sertoli Cells

(A) Immunostaining for GATA4 and m^{6}A or WTAP and SOX9 in testis cross sections from the indicated genotypes at P6. The arrows indicate Sertoli cells. Scale bars represent 20 μm.

(B–E) Testes (B) of control and *Wtap*-sKO male mice at P180. Scale bar represents 2 mm. Testis/body weight ratios at P6, P14, P21, P28, P35, P60, P120, and P180 (C), litter sizes from P60 to P150 (D), and sperm counts of cauda epididymis at P180 (E) from the indicated

(legend continued on next page)

seminiferous tubules also demonstrated that morphology and number of round and elongated spermatids in *Wtap*-sKO mice were comparable with those of control littermates at postnatal days 28 (P28) (Figures S3A and S3B).

We examined meiotic progression using spermatocyte nuclear spreading and the results indicated percentage of germ cells in leptotene, zygotene, pachytene, diplotene, and diakinesis were similar in testes of *Wtap*-sKO and control animals (Figures S3C and S3D). Formation of synaptonemal complex and progression of meiotic prophase did not show defects. Furthermore, integrity of the blood-testis barrier, an important ultrastructure essential for spermatogenesis, was not affected by *Wtap* loss-of-function (Figure S3E). Reduced testis/body weight ratio was observed in *Wtap*-sKO males and began as early as P21 (Figure 2C), and total germ cell number was reduced from P21 (Figures S4A and S4B). Together, these data revealed that the sterile phenotype of *Wtap*-sKO mice was caused by reduced sperm concentration because of germ cell loss.

Sertoli Cell-Specific Deletion of *Wtap* Caused Progressive Loss of Undifferentiated Spermatogonia

To identify the underlying reasons for germ cell loss, we examined the process of germ cell development in *Wtap*-sKO and control testes. H&E analyses showed that formation of spermatogonial lineage and development of spermatocytes and round spermatids were similar in testes of *Wtap*-sKO and control animals. Degeneration of seminiferous tubules was detectable beginning at P35 and the condition became severe with aging (Figure 2F). Immunofluorescence staining confirmed that some of these tubules only contained Sertoli cells without GCNA1$^+$ germ cells, suggesting the development of Sertoli cell-only (SCO) phenotype (Figure 2G). Quantitative analysis revealed that the percentages of degenerated tubules and SCO tubules increased with aging. Degenerated spermatogenesis was found in 83.0% of tubules and 49.3% of these tubules were SCO in *Wtap*-sKO mice at P180 (Figure 2H).

Next, we quantified the number of undifferentiated spermatogonia at different development stages. The ratio of LIN28A$^+$ undifferentiated spermatogonia per SOX9$^+$ cell did not change at P6, suggesting that formation of the undifferentiated spermatogonial pool was not affected by deleting *Wtap* in Sertoli cells. A significant reduction of undifferentiated spermatogonial population was found in *Wtap*-sKO mice at P21. Although the size of the Sertoli cell population did not change (Figure S4C), number of LIN28A$^+$ spermatogonia continued to decrease from P21 to P180 (Figures 2I and 2J). The whole-mount staining of seminiferous tubules for GFRA1 and FOXO1 revealed a significant reduction of A_{single} (A_s) spermatogonia, the primitive spermatogonia containing enriched SSCs in testes of *Wtap*-sKO mice (Figure 3A). Findings of these experiments indicated that deletion of *Wtap* in Sertoli cells resulted in a progressive loss of SSCs and depletion of germ cells.

Sertoli Cell-Derived WTAP Is Essential for SSC Self-renewal and Proliferation

To further determine the fate decisions of undifferentiated spermatogonia, we examined apoptosis, proliferation, and differentiation of A_s, A_{paired} (A_{pr}), and $A_{aligned}$ (A_{al}) undifferentiated spermatogonia. Firstly, we ruled out the possibility that SSC loss was due to apoptosis, because TUNEL (terminal deoxynucleotidyl transferase-mediated dUTP nick-end labeling) assay confirmed that apoptotic spermatocytes increased modestly in testes of *Wtap*-sKO mice (Figures S4D–S4F); however, undifferentiated spermatogonia rarely underwent apoptosis either in control or *Wtap*-sKO mice (Figure 3B). Next, we labeled proliferative cells with 5-ethynyl-2′-deoxyuridine (EdU) in control and *Wtap*-sKO animals at P14 and quantified the number of EdU$^+$ undifferentiated spermatogonia after 2 h or 7 days. The results uncovered that mitotic division was severely impaired in undifferentiated spermatogonia of *Wtap*-sKO mice. Particularly, EdU incorporation and retention rates in LIN28A$^+$ A_s spermatogonia were significantly reduced in *Wtap*-sKO mice compared with those of controls (Figures 3C and 3D). Similarly, GFRA1$^+$ A_s spermatogonia were sharply decreased in testis of *Wtap*-sKO mice (Figures S5A and S5B). To confirm that the SSC activity was indeed decreased, we performed a transplantation experiment to examine the SSC number in magnetic-activated cell sorted (MACS) THY1$^+$ from 4-week-old control and *Wtap*-sKO donors. LacZ-expressing ROSA26 line (ROSA26-lacZ) was

genotypes. At least three mice were used for each time point (n = 3 different animals). Ten control or *Wtap*-sKO animals were used in fertility test (n = 10 different animals). **p < 0.01 and ***p < 0.001.

(F–J) H&E staining of seminiferous tubules (F) from control and *Wtap*-sKO males at P6, P35, P60, and P180. Asterisks indicate SCO tubules. H&E staining and SOX9 and GCNA1 immunostaining (G) of SCO tubules from *Wtap*-sKO males. Quantification of seminiferous tubules from *Wtap*-sKO testes containing degenerated spermatogenesis and SCO phenotype (H) at P35, P60, P120, and P180. Immunostaining of LIN28A and SOX9 (I) in control and *Wtap*-sKO testes at P6, P35, P60, and P180. Statistics of the number of LIN28A$^+$ cells per SOX9$^+$ cell (J) from the indicated genotypes at P6, P21, P35, P60, and P180. At least 1500 SOX9$^+$ cells were counted per genotype at each time point. Scale bars represent 40 μm. Three animals were used for control or *Wtap*-sKO at each time point (n = 3 different animals). **p < 0.01 and ***p < 0.001.

See also Figures S2–S4.

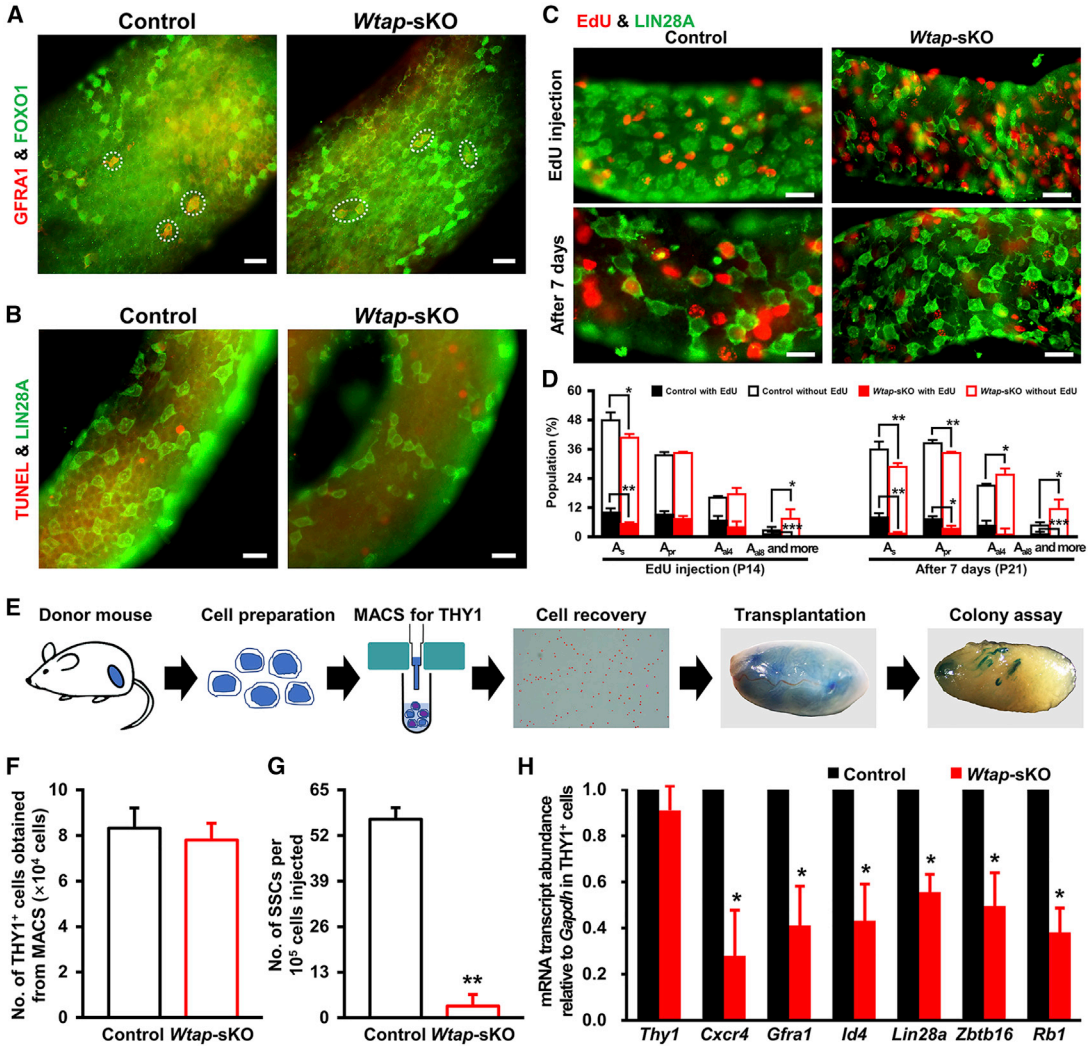

Figure 3. Impaired SSC Self-renewal and Proliferation Caused by *Wtap* Deletion in Mouse Sertoli Cells

(A–D) Whole-mount immunostaining of GFRA1 and FOXO1 (A) and TUNEL and LIN28A (B) in control and *Wtap*-sKO seminiferous tubules at P21. Whole-mount immunostaining of EdU and LIN28A (C) in control and *Wtap*-sKO seminiferous tubules after 2 h or 7 days post EdU injection at P14. Quantifications of EdU$^+$ A_s, A_{pr}, and A_{al} spermatogonia in Lin28A$^+$ cells (D) of control and *Wtap*-sKO testes. At least 900 LIN28A$^+$ cells were counted per genotype for each time point. Three animals were used for control or *Wtap*-sKO at each time point (n = 3 different animals). *p < 0.05, **p < 0.01, and ***p < 0.001. Scale bars represent 40 μm.

(E–G) The schematic diagram (E) of germ cell transplantation experiment. Quantification of THY1$^+$ cells obtained using MACS (F) and SSC numbers in THY1$^+$ undifferentiated spermatogonia (G) from control and *Wtap*-sKO males. SSC numbers were derived from donor-derived colonies of spermatogenesis in recipient testes and normalized to 10^5 cells injected. THY1$^+$ cells from three control or *Wtap*-sKO animals (4 weeks old) were isolated and transplanted into testes of six recipients (n = 3 different animals). **p < 0.01.

(H) qRT-PCR analysis of *Thy1*, *Cxcr4*, *Gfra1*, *Id4*, *Lin28*, *Zbtb16*, and *Rb1* transcript abundances in THY1$^+$ cells from control and *Wtap*-sKO testes. Four control or *Wtap*-sKO animals were used (n = 4 different animals). *p < 0.05.

See also Figures S4 and S5.

crossed with control or *Wtap*-sKO animals to label donor-derived spermatogenesis (Figure 3E). The numbers of THY1$^+$ cells recovered from control and *Wtap* conditional knockout animals were comparable (Figure 3F) and a 10-μL single-cell suspension (containing 10^4 THY1$^+$ cells) was transplanted into one testis of busulfan-treated recipients. The recipients were examined 8 weeks after transplantation for donor-derived spermatogenesis by X-Gal staining as previously described (Kubota et al., 2004; Yang et al., 2013). The average number of donor-cell-derived colonies was 56.7 colonies/10^5 cells injected for control animals; however, the same number of donor cells only

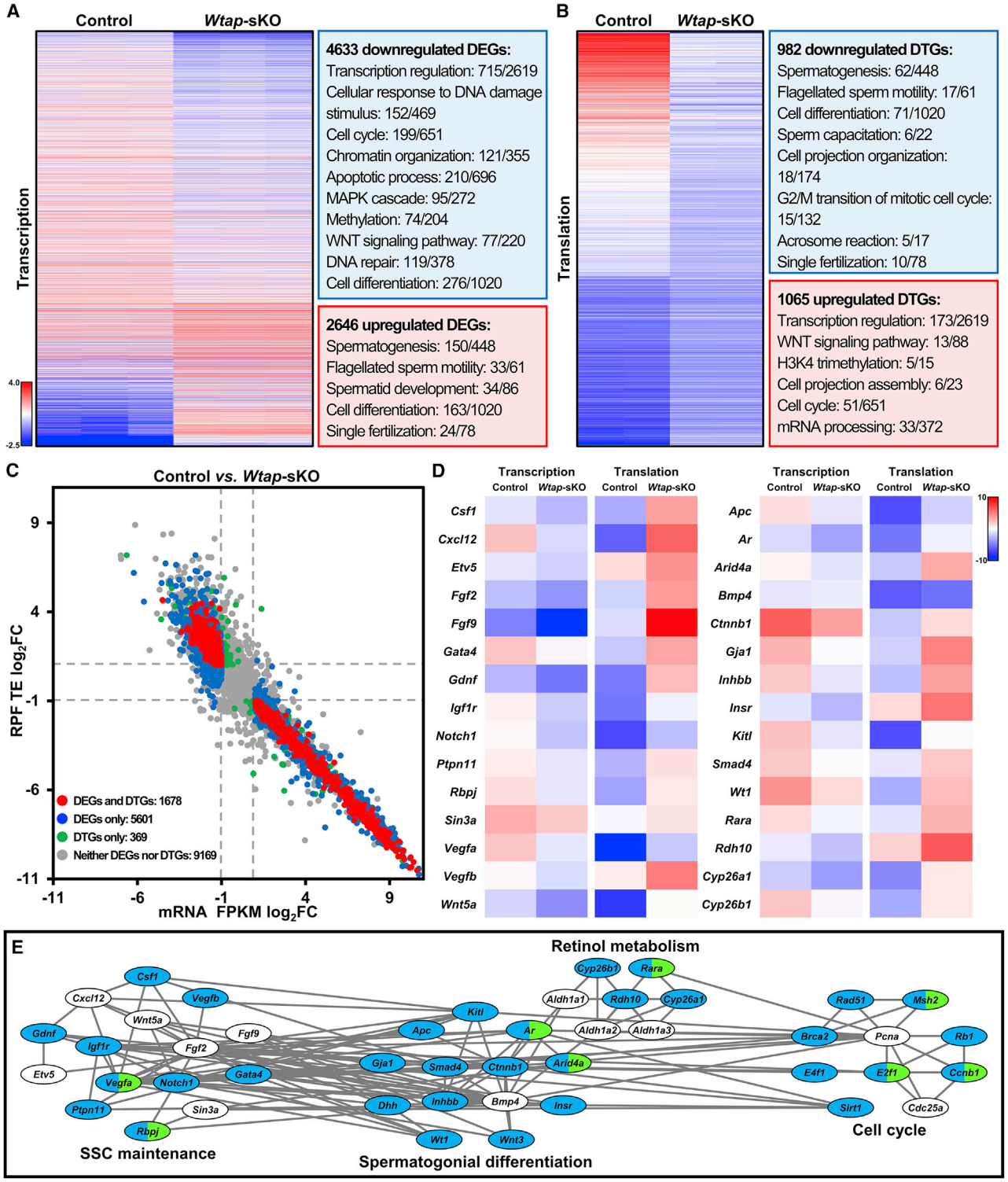

Figure 4. Transcriptional and Translational Dysregulations in Sertoli Cells from *Wtap*-sKO Mice

(A and B) Heat map showing the DEGs (A) and DTGs (B) between control and *Wtap*-sKO animals and their function enrichment. Gene differences with $|\log_2 \text{fold change}| \geq 1$ and $p < 0.01$ are identified as significant. The enriched biological process GO terms in down-regulated (blue boxes) and upregulated (red boxes) genes upon *Wtap* knockout are shown in the right panels.

(legend continued on next page)

generated 3.3 colonies for *Wtap*-sKO animals, indicating SSC activities were affected dramatically by *Wtap* deletion in Sertoli cells (Figure 3G). We next investigated relative abundance of factors related to SSC maintenance, and the data revealed that expressions of *Cxcr4*, *Gfra1*, *Id4*, *Lin28a*, *Zbtb16*, and *Rb1* were greatly reduced in THY1$^+$ germ cells from *Wtap*-sKO males; however, *Thy1* expression did not show difference (Figure 3H). Lastly, we quantified number of differentiating spermatogonia by immunofluorescent staining for KIT or STRA8 and found that the number of KIT$^+$ germ cells was decreased at P21 in testes of *Wtap*-sKO mice (Figures S5C and S5D). Interestingly, number of STRA8 and LIN28A double-positive cells (STRA8$^+$ and LIN28A$^+$) was significantly decreased in *Wtap*-sKO mice (Figures S5E–S5G), indicating that spermatogonial differentiation was impaired. From these data, we concluded that deletion of *Wtap* in Sertoli cells caused major defects in SSC self-renewal/proliferation. *Wtap* deletion also affected the spermatogonial differentiation. Together, findings of these studies demonstrated that, without critical roles of WTAP, Sertoli cells failed to provide a functional niche to support SSC fate decisions properly, leading to the exhaustion of SSC pool.

Wtap Deletion Altered Gene Transcription and Translation in Sertoli Cells

To understand how WTAP functions to maintain a healthy SSC niche, we conducted high-throughput RNA sequencing (RNA-seq) and ribosome nascent-chain complex-bound mRNA sequencing (RNC-seq) to evaluate changes in gene expression at transcriptional and translational levels in WTAP-null Sertoli cells. RNA-seq revealed that a total of 7,279 (2,646 up and 4,633 down) mRNA were differentially expressed genes (DEGs) in WTAP-deficient Sertoli cells. GO analysis indicated that downregulated transcripts were involved in transcription regulation, cellular response to DNA damage stimulus, cell cycle, chromatin organization, apoptosis process, MAPK cascade, methylation, WNT signaling pathway, DNA repair, and cell differentiation (Figure 4A and Table S4). RNC-seq data identified a list of 2,047 (1,065 up and 982 down) differentially translated genes (DTGs) evaluated by TE, normalized read count of ribosome-protected fragments (RPF)/mRNA fragments. Upregulated DTGs were involved in transcription regulation, WNT signaling pathway, H3K4 trimethylation, cell projection assembly, cell cycle, and mRNA processing (Figure 4B and Table S4). Notably, 81.97% (1,678/2,047) of DTGs were found in DEGs, and 789 transcriptionally downregulated genes were translationally upregulated while 880 transcriptionally upregulated genes were translationally downregulated (Figure 4C). Transcripts previously shown to be important for SSC maintenance, spermatogonial differentiation, and Sertoli cell fate decisions were dysregulated (Figure 4D). Of particular interest, we found that transcript abundances of *Igf1r*, *Vegfa*, *Notch1*, *Csf1*, *Gdnf*, *Ptpn11*, *Rbpj*, *Gata4*, *Vegfb*, *Smad4*, *Inhbb*, *Ctnnb1*, *Kitl*, *Apc*, *Gja1*, *Dhh*, *Wt1*, *Wnt3*, *Insr*, *Arid4a*, *Ar*, *Rdh10*, *Cyp26b1*, *Cyp26a1*, *Rara*, *E2f1*, *Rad51*, *Brca2*, *E4f1*, *Sirt1*, *Ccnb1*, *Rb1*, and *Msh2* were altered. Among them, *Vegfa*, *Rbpj*, *Arid4a*, *Ar*, *Rara*, *E2f1*, *Ccnb1*, and *Msh2* were translationally dysregulated (Figure 4E). Together, these data uncovered roles of WTAP in regulating gene expression in Sertoli cells at transcriptional and translational levels.

Wtap Deletion Changed Transcription and Translation of m^{6}A-Enriched Transcripts in Sertoli Cells

To further understand how WTAP-dependent m^{6}A modifications were involved in sustaining the SSC niche, RNA-seq, RNC-seq, and m6A sequencing (m^{6}A-seq) were comprehensively analyzed to decipher patterns of gene regulation in Sertoli cells. As expected, expressions of m^{6}A-enriched transcripts were significantly affected by *Wtap* deletion; 37.59% (2,736/7,279) of DEGs and 37.13% (760/2047) of DTGs were m^{6}A-enriched, and more m^{6}A sites were enriched in transcriptionally downregulated and translationally upregulated genes (Figures 5A and 5B). It is noteworthy that DEGs with m^{6}A showed higher expression levels than those without m^{6}A in control Sertoli cells and exhibited sharper changes upon *Wtap* knockout (Figure 5C). Importantly, many transcripts that encode proteins to be important for m^{6}A modifications were downregulated in WTAP-deficient Sertoli cells (Figure 5D), indicating a core role of WTAP in m^{6}A formation in Sertoli cells. Reads distribution analyses of representative genes (*Cxcl12* and *Csf1*) revealed remarkable transcriptional changes within m^{6}A sites on mRNA reads, while translating mRNA was less affected (Figure 6A).

(C) Scatterplots showing the relationship of fold changes between mRNA FPKM and RPF TE of genes in Sertoli cells upon *Wtap* knockout. Red, blue, green, and gray plots indicate genes belonging to both DEGs and DTGs, DEGs only, DTGs only, and neither DEGs nor DTGs.
(D) Heat maps showing the relative levels of mRNA FPKM and RPF TE of genes involving SSC maintenance and spermatogonial differentiation in Sertoli cells.
(E) Interaction network showing genes involved in spermatogenesis regulation. Two genes with regulatory relationships are connected directly, DEGs and DTGs are marked in blue and green respectively.
All analyses were performed on three different control or *Wtap*-sKO samples (n = 3 different biological replicates). *$p < 0.05$. See also Table S4.

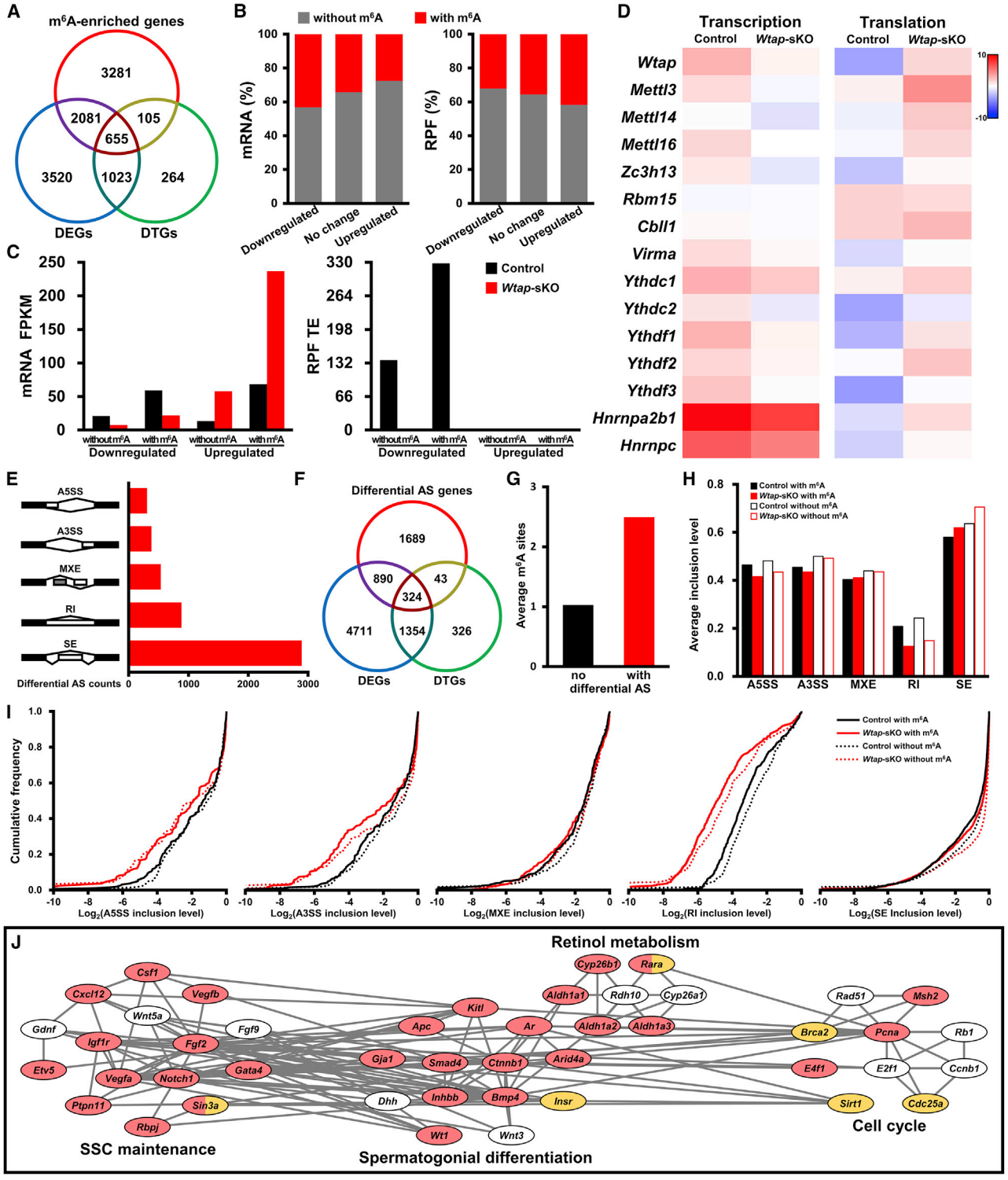

Figure 5. Effects of WTAP-Mediated m^{6}A Modification on Transcriptional and Post-transcriptional Regulation of Sertoli Cell Gene Expression

(A–D) Venn diagram showing numbers of DEGs and DTGs with or without m^{6}A modification (A), proportions of m^{6}A-enriched genes on differential transcriptional and translational changes (B), mRNA FPKM of DEGs and RPF TE of DTGs with or without m^{6}A modification (C), and heat maps showing relative levels of mRNA FPKM and RPF TE of the main m^{6}A regulators (D) in control and *Wtap*-sKO Sertoli cells.

(legend continued on next page)

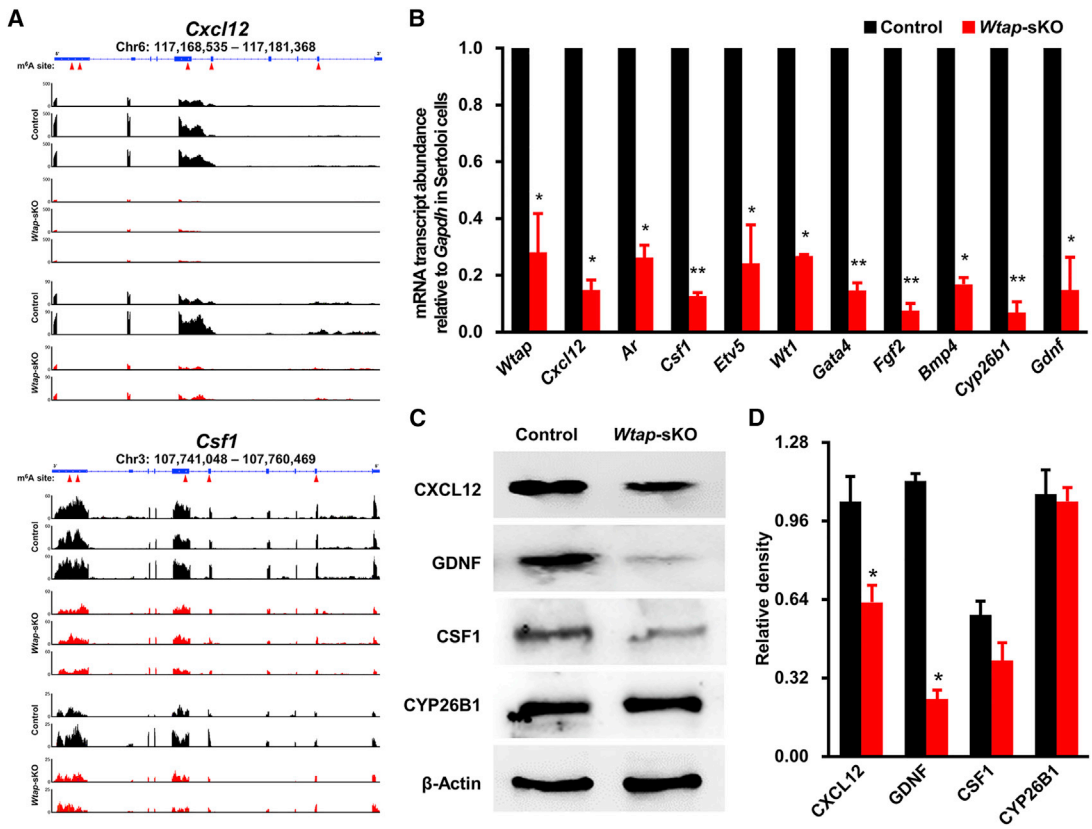

Figure 6. Decreased Expression of SSC Niche Factors Caused by *Wtap* Deletion

(A) mRNA and RNC mRNA reads of *Cxcl12* and *Csf1* in control and *Wtap*-sKO samples. The m^{6}A sites are marked as red triangles.

(B) qRT-PCR analysis of *Wtap*, *Cxcl12*, *Ar*, *Csf1*, *Etv5*, *Wt1*, *Gata4*, *Fgf2*, *Bmp4*, *Cyp26b1*, and *Gdnf* transcript abundances in control and *Wtap*-sKO Sertoli cells.

(C and D) Western blot (C) and quantitative data (D) showing CXCL12, GDNF, CSF1, and CYP26B1 expression in control and *Wtap*-sKO testes.

All quantitative data are presented as the mean ± SEM for n = 3 independent biological replicates. *p < 0.05 and **p < 0.01.

Several lines of evidences uncovered that m^{6}A modification regulates pre-mRNA splicing (Adhikari et al., 2016), so we next examined alternative splicing (AS) events in control and *Wtap*-sKO Sertoli cells. In total, 5,003 differential AS events in 2,946 genes were detected, and skipped exon (SE) accounted for 57.87% (2,895/5,003) of the total (Figure 5E and Table S5). Venn diagrams showed that 1,214 DEGs and 367 DTGs contained splicing variants (Figure 5F). As expected, genes with differential AS events displayed abundant m^{6}A enrichment (Figure 5G). The effect of m^{6}A on AS events was further analyzed and the results showed that alternative 5′ splice site (A5SS) remained almost entirely unaffected by m^{6}A modification, while differences in alternative 3′ splice site (A3SS) were apparent in mRNA with and without m^{6}A modification. Interestingly, great influences of m^{6}A modification on alternative exons including SE, mutually exclusive exons (MXEs), and retained introns (RIs) were evident (Figures 5H and 5I). Interaction network identified a list of genes that were showed to be important for Sertoli cell function. Most of them

(E–I) Statistics of five types of differential AS events (E) on mRNA transcripts in control and *Wtap*-sKO Sertoli cells. Venn diagram (F) showing numbers of DEGs and DTGs with or without differential AS events in Sertoli cells. Average m^{6}A sites (G) of genes with or without differential AS events. Average inclusion levels (H) and cumulative frequency curves for inclusion levels (I) of A5SS and A3SS, MXE, RI, and SE in genes with or without m^{6}A modification between control and *Wtap*-sKO animals.

(J) Interaction network showing genes involved in spermatogenesis regulation. Two genes with regulatory relationships are connected directly, genes with m^{6}A modification and differential AS events are marked in red and yellow respectively.

All analyses were performed on three different control or *Wtap*-sKO samples (n = 3 different biological replicates). *p < 0.05. See also Table S5.

were m^{6}A-enriched, including *Igf1r*, *Vegfa*, *Notch1*, *Fgf2*, *Csf1*, *Cxcl12*, *Etv5*, *Ptpn11*, *Rbpj*, *Sin3a*, *Gata4*, *Vegfb*, *Smad4*, *Inhbb*, *Bmp4*, *Ctnnb1*, *Kitl*, *Apc*, *Gja1*, *Wt1*, *Arid4a*, *Ar*, *Cyp26b1*, *Aldh1a1*, *Aldh1a2*, *Aldh1a3*, *Rara*, *Pcna*, *E4f1*, and *Msh2*. In addition, AS events were detected in *Sin3a*, *Insr*, *Rara*, *Brca2*, *Sirt1*, and *Cdc25a* (Figure 5J). These analyses indicated that changes in m^{6}A modifications alter transcription and translation of genes that are important for fate decisions of SSCs and their progenitors; for example, *Cxcl12* and *Csf1* (Figure 6A). To validate these findings, we examined relative expression of *Cxcl12*, *Csf1*, *Etv5*, *Wt1*, *Fgf2*, *Bmp4*, and other downregulated transcripts using qRT-PCR (Figure 6B) and these results were consistent with RNA-seq. We also examined protein levels of CXCL12, GDNF, CSF1, and CYP26B1 in testis from control and *Wtap*-sKO animals and the results showed that CXCL12, GDNF, and CSF1 protein were reduced sharply by *Wtap* loss-of-function in Sertoli cells (Figures 6C and 6D). Together, these data demonstrated that WTAP-mediated m^{6}A regulates AS events of genes regulating SSC niche and spermatogonial fate decisions.

DISCUSSION

m^{6}A is a highly conserved internal RNA modification that influences gene expression at transcriptional and post-transcriptional levels (Gilbert et al., 2016). Recent studies revealed crucial roles of m^{6}A in stem cell fate decisions (Cheng et al., 2019; Geula et al., 2015); however, its dynamics and functions in stem cell and niche interactions remained largely unknown. Because WTAP is a key member of m^{6}A modification complex (Ping et al., 2014) and highly expressed in Sertoli cells, here, we illustrate the m^{6}A methylome landscape of Sertoli cells in murine testis and demonstrate that WTAP-mediated m^{6}A modification is a key regulatory mechanism that instructs the expression of SSC niche factors at the transcriptional and translation levels in Sertoli cells.

We describe patterns of m^{6}A methylome in mouse Sertoli cells and provide an important reference for further deciphering functions of transcripts with m^{6}A modification in mediating molecular interactions between stem cells and their niches. Sertoli cells are major cellular components of the SSC niche (Oatley and Brinster, 2012); however, regulatory mechanisms that specify and maintain the SSC niche are not well understood. In this study, we found m^{6}A modification in Sertoli cells is different from spermatogenic cells as previously described (Lin et al., 2017).The number of m^{6}A peak sites of Sertoli cells was similar to that of spermatogonia and greater than that of spermatocytes or round spermatids, while the number of m^{6}A peak sites of Sertoli cells identifeid in this study was similar to that of round spermatids and significantly less than that of spermatogonia. These finding support the conclusion that transcripts of Sertoli cells harbor intense m^{6}A modification, and m^{6}A-enriched transcripts serve different roles in governing normal spermatogenesis.

Transcripts of previously identified SSC niche factors and transcription regulators important for the development of spermatogenic lineage are m^{6}A enriched. CXCL12 and CSF1 are important niche factors that enhance SSC self-renewal (Oatley et al., 2009; Yang et al., 2013). VEGFA, FGF2, and PDGFB are growth factors in the niche milieu that influence SSC fate decisions (Basciani et al., 2008; Ishii et al., 2012; Lu et al., 2013). Activation of NOTCH signaling in Sertoli cells increases the expression of GDNF and stimulates SSC expansion (Garcia et al., 2014). BMP4 and KITL direct spermatogonial differentiation (Ohta et al., 2000; Yang et al., 2016). ARID4A and ARID4B interact with RB1 to regulate Sertoli cell function and spermatogenesis (Wu et al., 2013); importantly, deletion of *Arid4b* in Sertoli cells affects the establishment of SSC niche in mouse (Wu et al., 2017). *Wt1* deletion in neonatal Sertoli cells results in the accumulation of undifferentiated spermatogonia due to defects in spermatogonial differentiation and meiosis (Zheng et al., 2014). SIN3A-deficient Sertoli cells cannot support long-term maintenance of the spermatogonial population and normal development of spermatids (Payne et al., 2010). Functional roles of other transcripts in influencing the initial formation and maintenance of the SSC niche await further investigations.

In this study, we demonstrate that WTAP function in Sertoli cells serves specific roles in dictating SSC fate decisions. WTAP was first identified as a WT1-binding partner and WT1 mainly functions as a key regulator of somatic lineage specification in fetal gonad (Chen et al., 2017); in sharp contrast, *Wtap* deletion results in the exhaustion the SSC pool without affecting meiosis or spermiogenesis. We did not observe defects in the gonocyte to spermatogonial transition in the neonatal testis of *Wtap* conditional knockout animals, suggesting the initial establishment of the SSC niche is not affected. It is commonly observed that Sertoli cell dysfunctions affect development of meiotic and post-meiosis germ cells (O'Shaughnessy, 2014), and, to our knowledge, transcriptional or translational factor in Sertoli cells that only controls the fate of SSC has not been reported; therefore, our findings revealed a novel role of WTAP in determining the long-term maintenance of the SSC niche. Phenotypic and mechanistic analyses support the idea that WTAP machinery provides a microenvironment that ensures the balance between SSC self-renewal and differentiation.

WTAP regulates transcription and translation of niche factors by depositing the m^{6}A marks directly on transcripts encoding the niche factors or indirectly on transcription

regulators. Although WTAP deficiency dramatically induces transcriptional and translational changes of a large number of genes in Sertoli cells, we found that most significantly affected transcripts are involved in SSC maintenance, spermatogonial differentiation, retinol metabolism, and cell cycle. *Gdnf*, the essential factor required for SSC maintenance, is not marked by m^{6}A modification; however, its expression level was downregulated upon *Wtap* deletion. Interestingly, several of the key transcription regulators that have been reported to be important for *Gdnf* transcription contained m^{6}A sites and were dysregulated by *Wtap* knockout. Biogenesis of retinoic acid (RA) is strictly controlled in Sertoli cells (Teletin et al., 2019) and RA signaling interacts with the niche factors to influence the fate of undifferentiated spermatogonia (Yang et al., 2013); therefore, it is not surprising that transcripts involved in RA metabolism and functions are modified by m^{6}A and dysregulated by *Wtap* deletion.

A major function of WTAP is to control mRNA splicing in Sertoli cells. m^{6}A is established using S-adenosyl methionine as substrate, and catalyzed by m^{6}A methyltransferases "writers" and recognized by m^{6}A binding proteins "readers" to induce subsequent reactions (Balacco and Soller, 2019). In germ cells, deletion of m^{6}A reader *Ythdc1* leads to the loss of germ cells including mitotic spermatogonia (Kasowitz et al., 2018) and deletion of *Ythdc2* causes defects in meiosis (Hsu et al., 2017; Wojtas et al., 2017). Deletion of m^{6}A writer *Mettl3* or *Mettl14* inhibits SSC proliferation/differentiation and combined ablation of them in advanced germ cells disrupts spermiogenesis (Lin et al., 2017). Notably, these m^{6}A methylases all affected mRNA splicing. WTAP is an evolutionarily conserved regulator of AS events that functions in post-transcriptional regulation, including mRNA splicing, stabilization, polyadenylation, and export (Horiuchi et al., 2013). WTAP interacts with METTL3 and METTL14 through the anchoring effect of ZC3H13 to control AS events and m^{6}A formation (Wen et al., 2018). In the present study, we illustrate that loss of WTAP function in Sertoli cells produced a pronounced variation in splicing events and a great amount of A3SS, SE, MXE, and RI occurred in m^{6}A-enriched genes. The alteration of splicing events in spermatogenesis-regulating genes caused by m^{6}A deprivation could be one of the core reasons for defective spermatogenesis.

Collectively, our results demonstrate that WTAP-mediated m^{6}A modification controls mRNA transcription and translation to orchestrate the gene expressions in Sertoli cells that are essential for SSC maintenance and spermatogonial differentiation. These findings provide new insights into molecular regulation of the SSC niche, and results of the present study may be helpful in deciphering interactions between stem cells and their cognate niches in other mammalian systems.

EXPERIMENTAL PROCEDURES

Mice

The *Wtap* knockout first embryonic stem cells (C57BL/6N-*Wtap*$^{<tm1a(EUCOMM)Hmgu>/H}$, hereafter *Wtap*^{tm1a}) were obtained from MRC Harwell Institute (Oxford, UK). In the knockout first allele, a promoter-driven cassette (including *LacZ* and *neo* genes) flanked by *FRT* sites are inserted between exon 3 and exon 4, whereas the exon 4 and exon 5 of *Wtap* are flanked by *LoxP* sites. We converted the knockout first allele to a conditional allele by crossing *Wtap*^{tm1a} mice with Flp deleter mice. The resulting floxed *Wtap* were crossed with *Amh-Cre* mice obtained from Jackson Laboratory (Maine, US) to allow specific knockout of *Wtap* in Sertoli cells. Obtained mice were genotyped with the tail DNA. All primers for genotyping are listed in the Table S6. The *Sox9*^{Gfp} mice used for isolation of highly purified Sertoli cells were obtained from Mutant Mouse Resource & Research Centers (MMRRC_011019-UCD). The C57BL/6N mice used for isolation of a large number of Sertoli cells and 129S2/SvPasCrl mice used for transplantation experiments were purchased from Vital River Laboratory Animal Center (Beijing, China) and housed in the animal facilities of Northwest Institute of Plateau Biology, Chinese Academy of Sciences. All animal experiments were approved by the Animal Ethic and Welfare Committee at Northwest Institute of Plateau Biology, Chinese Academy of Sciences.

m^{6}A-seq

m^{6}A-seq was performed as previously described (Lin et al., 2017). Briefly, mRNA isolated from Sertoli cells was enriched using SeqStar Poly(A) mRNA Isolation Kit. mRNA was fragmented to ~100 nt and mixed with affinity-purified anti-m^{6}A antibody for immunoprecipitation (IP). The eluted RNA was resuspended and used for library preparation with KAPA Stranded RNA-seq Kit. Sequencing was carried out on Illumina HiSeq 4000 using an 8 pM template per sample for cluster generation with HiSeq 3000/4000 SBS Kit by KangChen Biotechnology Co., Ltd. (Shanghai, China).

After controlling quality by FastQC and removing adapters and low-quality reads by Trimmomatic (Bolger et al., 2014), sequencing reads were aligned to the reference genome (mm10) using HISAT2 (Kim et al., 2015). The longest isoform was used if the gene had multiple isoforms. The m^{6}A peaks were detected by exomePeak (Meng et al., 2014) and windows with read counts <1/20 of the top window in both m^{6}A IP and input samples were excluded. The differential windows were identified between m^{6}A IP and input samples using edgeR (Robinson et al., 2010), and the enrichment score of each window was calculated as previously described (Lin et al., 2017). The window was called positive if enrichment score was >1 and $p < 0.01$.

RNA-seq and RNC-seq in Parallel

The isolated Sertoli cells were resolved in prechilled TRIzol for RNA-seq or fixed buffer (0.3 mg/mL antibiotic inhibitor and 50 mM $MgCl_2$ in PBS) for RNC-seq and stored at −80°C immediately after liquid nitrogen freeze. RNC mRNA was enriched by sucrose density centrifugation to obtain full-length mRNA on

ribosome as described (Wang et al., 2013). Then, total RNA and RNC mRNA were isolated respectively, equal amounts of total RNA or RNC mRNA from each sample were prepared for subsequent library construction, and RNA-seq or RNC-seq following the same procedure, including fragmentation, reverse transcription, synthesis, purification, adaptor ligation, and PCR amplification. Libraries successfully constructed were sequenced using Illumina HiSeq2500.

Clean reads without adapters and low-quality bases were further processed to remove rRNA reads by Bowtie2 (Langmead and Salzberg, 2012). TopHat2 was used for mapping reads to reference genome (mm10) (Kim et al., 2013), and Cufflinks was used together for the reconstruction of transcripts (Trapnell et al., 2012). Gene abundance was quantified using RSEM (RNA-seq by expectation maximization) (Li and Dewey, 2011), and the gene expression level was normalized by fragments per kilobase of exon model per million reads mapped (FPKM). Genes with no less than 0.5 FPKM in at least one sample were used for subsequent analysis. For identifying DEGs at transcription level, edgeR was used, and genes with $|\log_2\text{fold change}| \geq 1$ and $p < 0.01$ between control and *Wtap*-sKO animals from RNA-seq were identified as significant DEGs. For digging DTGs between control and *Wtap*-sKO animals at translation level, TE was calculated based on normalized read count of RNC mRNA/mRNA and genes with $|\log_2\text{-fold change}| \geq 1$ and $p < 0.01$ between control and *Wtap*-sKO animals were identified as significant DTGs.

Data and Code Availability

The m6A-seq, RNA-seq, and RNC-seq data are available in the NCBI BioProject under accession numbers PRJNA661168 and PRJNA661226.

SUPPLEMENTAL INFORMATION

Supplemental Information can be found online at https://doi.org/10.1016/j.stemcr.2020.09.001.

AUTHOR CONTRIBUTIONS

Q.Y. devised and supervised this project. G.J., Z.L., R.Y., G.W., X.Z., and C.L. performed the experiments and bioinformatics analysis. Q.Y., G.J., and M.T. wrote the manuscript with contributions from all authors.

ACKNOWLEDGMENTS

The work was supported by the National Natural Science Foundation of China (grants nos. 31571539, 31771656, and 31930034) and Natural Science Foundation of Qinghai Province (2020-ZJ-902). Q.Y. was supported by Chinese Academy of Sciences (CAS) "100 Talents" and Qinghai "1000 Talents" programs. G.J. was supported by CPSF-CAS Joint foundation for Postdoctoral Fellows and "CAS Light of West" programs.

Received: January 1, 2020
Revised: September 5, 2020
Accepted: September 7, 2020
Published: October 13, 2020

REFERENCES

Adhikari, S., Xiao, W., Zhao, Y.L., and Yang, Y.G. (2016). m^6A: signaling for mRNA splicing. RNA Biol. *13*, 756–759.

Balacco, D.L., and Soller, M. (2019). The m^6A writer: rise of a machine for growing tasks. Biochemistry *58*, 363–378.

Basciani, S., De Luca, G., Dolci, S., Brama, M., Arizzi, M., Mariani, S., Rosano, G., Spera, G., and Gnessi, L. (2008). Platelet-derived growth factor receptor β-subtype regulates proliferation and migration of gonocytes. Endocrinology *149*, 6226–6235.

Bolger, A.M., Lohse, M., and Usadel, B. (2014). Trimmomatic: a flexible trimmer for Illumina sequence data. Bioinformatics *30*, 2114–2120.

Chen, M., Zhang, L.J., Cui, X.H., Lin, X.W., Li, Y.Q., Wang, Y.Q., Wang, Y.B., Qin, Y., Chen, D.H., Han, C.S., et al. (2017). *Wt1* directs the lineage specification of Sertoli and granulosa cells by repressing *Sf1* expression. Development *144*, 44–53.

Cheng, Y.M., Luo, H.Z., Izzo, F., Pickering, B.F., Nguyen, D., Myers, R., Schurer, A., Gourkanti, S., Bruning, J.C., Vu, L.P., et al. (2019). m^6A RNA methylation maintains hematopoietic stem cell identity and symmetric commitment. Cell Rep. *28*, 1703–1716.

De Rooij, D.G. (2017). The nature and dynamics of spermatogonial stem cells. Development *144*, 3022–3030.

De Rooij, D.G. (1988). Regulation of the proliferation of spermatogonial stem cells. J. Cell Sci. *10*, 181–194.

Fujihara, Y., Satouh, Y., Inoue, N., Isotani, A., Ikawa, M., and Okabe, M. (2012). SPACA1-deficient male mice are infertile with abnormally shaped sperm heads reminiscent of globozoospermia. Development *139*, 3583–3589.

Garcia, T.X., Farmaha, J.K., Kow, S., and Hofmann, M.C. (2014). RBPJ in mouse Sertoli cells is required for proper regulation of the testis stem cell niche. Development *141*, 4468–4478.

Geula, S., Moshitch-Moshkovitz, S., Dominissini, D., Mansour, A.A., Kol, N., Salmon-Divon, M., Hershkovitz, V., Peer, E., Mor, N., Manor, Y.S., et al. (2015). m^6A mRNA methylation facilitates resolution of naive pluripotency toward differentiation. Science *347*, 1002–1006.

Gilbert, W.V., Bell, T.A., and Schaening, C. (2016). Messenger RNA modifications: form, distribution, and function. Science *352*, 1408–1412.

Green, C.D., Ma, Q.Y., Manske, G.L., Shami, A.N., Zheng, X.N., Marini, S., Moritz, L., Sultan, C., Gurczynski, S.J., Moore, B.B., et al. (2018). A comprehensive roadmap of murine spermatogenesis defined by single-cell RNA-seq. Dev. Cell *46*, 651–667.

Griswold, M.D. (1998). The central role of Sertoli cells in spermatogenesis. Semin. Cell Dev. Biol. *9*, 411–416.

Griswold, M.D. (2018). 50 years of spermatogenesis: Sertoli cells and their interactions with germ cells. Biol. Reprod. *99*, 87–100.

Horiuchi, K., Umetani, M., Minami, T., Okayama, H., Takada, S., Yamamoto, M., Aburatani, H., Reid, P.C., Housman, D.E., Hamakubo, T., et al. (2006). Wilms' tumor 1-associating protein regulates G_2/M transition through stabilization of cyclin A2 mRNA. Proc. Natl. Acad. Sci. U S A *103*, 17278–17283.

Horiuchi, K., Kawamura, T., Iwanari, H., Ohashi, R., Naito, M., Kodama, T., and Hamakubo, T. (2013). Identification of Wilms' tumor

1-associating protein complex and its role in alternative splicing and the cell cycle. J. Biol. Chem. *288*, 33292–33302.

Hsu, P.J., Zhu, Y.F., Ma, H.H., Guo, Y.H., Shi, X.D., Liu, Y.Y., Qi, M.J., Lu, Z.K., Shi, H.L., Wang, J.Y., et al. (2017). Ythdc2 is an N^6-methyladenosine binding protein that regulates mammalian spermatogenesis. Cell Res. *27*, 1115–1127.

Ishii, K., Kanatsu-Shinohara, M., Toyokuni, S., and Shinohara, T. (2012). FGF2 mediates mouse spermatogonial stem cell self-renewal via upregulation of *Etv5* and *Bcl6b* through MAP2K1 activation. Development *139*, 1734–1743.

Jones, D.L., and Wagers, A.J. (2008). No place like home: anatomy and function of the stem cell niche. Nat. Rev. Mol. Cell Biol. *9*, 11–21.

Kasowitz, S.D., Ma, J., Anderson, S.J., Leu, N.A., Xu, Y., Gregory, B.D., Schultz, R.M., and Wang, P.J. (2018). Nuclear m^6A reader YTHDC1 regulates alternative polyadenylation and splicing during mouse oocyte development. PLoS Genet. *14*, e1007412.

Kim, D., Pertea, G., Trapnell, C., Pimentel, H., Kelley, R., and Salzberg, S.L. (2013). TopHat2: accurate alignment of transcriptomes in the presence of insertions, deletions and gene fusions. Genome Biol. *14*, R36.

Kim, D., Langmead, B., and Salzberg, S.L. (2015). HISAT: a fast spliced aligner with low memory requirements. Nat. Methods *12*, 357–360.

Kobayashi, M., Ohsugi, M., Sasako, T., Awazawa, M., Umehara, T., Iwane, A., Kobayashi, N., Okazaki, Y., Kubota, N., Suzuki, R., et al. (2018). The RNA methyltransferase complex of WTAP, METTL3, and METTL14 regulates mitotic clonal expansion in adipogenesis. Mol. Cell. Biol. *38*, e00116-18.

Kubota, H., Avarbock, M.R., and Brinster, R.L. (2004). Culture conditions and single growth factors affect fate determination of mouse spermatogonial stem cells. Biol. Reprod. *71*, 722–731.

Langmead, B., and Salzberg, S.L. (2012). Fast gapped-read alignment with Bowtie 2. Nat. Methods *9*, 357–359.

Li, B., and Dewey, C.N. (2011). RSEM: accurate transcript quantification from RNA-seq data with or without a reference genome. BMC Bioinformatics *12*, 323.

Lin, Z., Hsu, P.J., Xing, X.D., Fang, J.H., Lu, Z.K., Zou, Q., Zhang, K.J., Zhang, X., Zhou, Y.C., Zhang, T., et al. (2017). Mettl3-/Mettl14-mediated mRNA N^6-methyladenosine modulates murine spermatogenesis. Cell Res. *27*, 1216–1230.

Liu, J.Z., Yue, Y.N., Han, D.L., Wang, X., Fu, Y., Zhang, L., Jia, G.F., Yu, M., Lu, Z.K., Deng, X., et al. (2014). A METTL3-METTL14 complex mediates mammalian nuclear RNA N^6-adenosine methylation. Nat. Chem. Biol. *10*, 93–95.

Lu, N.X., Sargent, K.M., Clopton, D.T., Pohlmeier, W.E., Brauer, V.M., McFee, R.M., Weber, J.S., Ferrara, N., Silversides, D.W., and Cupp, A.S. (2013). Loss of vascular endothelial growth factor A (VEGFA) isoforms in the testes of male mice causes subfertility, reduces sperm numbers, and alters expression of genes that regulate undifferentiated spermatogonia. Endocrinology *154*, 4790–4802.

Lukjanenko, L., Jung, M.J., Hegde, N., Perruisseau-Carrier, C., Migliavacca, E., Rozo, M., Karaz, S., Jacot, G., Schmidt, M., Li, L.J., et al. (2016). Loss of fibronectin from the aged stem cell niche affects the regenerative capacity of skeletal muscle in mice. Nat. Med. *22*, 897–905.

Meng, X., Lindahl, M., Hyvonen, M.E., Parvinen, M., De Rooij, D.G., Hess, M.W., Raatikainen-Ahokas, A., Sainio, K., Rauvala, H., Lakso, M., et al. (2000). Regulation of cell fate decision of undifferentiated spermatogonia by GDNF. Science *287*, 1489–1493.

Meng, J., Lu, Z.L., Liu, H., Zhang, L., Zhang, S.W., Chen, Y.D., Rao, M.K., and Huang, Y.F. (2014). A protocol for RNA methylation differential analysis with MeRIP-seq data and exomePeak R/Bioconductor package. Methods *69*, 274–281.

Mesa, K.R., Rompolas, P., and Greco, V. (2015). The dynamic duo: niche/stem cell interdependency. Stem Cell Reports *4*, 961–966.

O'Shaughnessy, P.J. (2014). Hormonal control of germ cell development and spermatogenesis. Semin. Cell Dev. Biol. *29*, 55–65.

Oatley, J.M., and Brinster, R.L. (2008). Regulation of spermatogonial stem cell self-renewal in mammals. Annu. Rev. Cell Dev. Biol. *24*, 263–286.

Oatley, J.M., and Brinster, R.L. (2012). The germline stem cell niche unit in mammalian testes. Physiol. Rev. *92*, 577–595.

Oatley, J.M., Oatley, M.J., Avarbock, M.R., Tobias, J.W., and Brinster, R.L. (2009). Colony stimulating factor 1 is an extrinsic stimulator of mouse spermatogonial stem cell self-renewal. Development *136*, 1191–1199.

Ohta, H., Yomogida, K., Dohmae, K., and Nishimune, Y. (2000). Regulation of proliferation and differentiation in spermatogonial stem cells: the role of c-kit and its ligand SCF. Development *127*, 2125–2131.

Payne, C.J., Gallagher, S.J., Foreman, O., Dannenberg, J.H., Depinho, R.A., and Braun, R.E. (2010). *Sin3a* is required by Sertoli cells to establish a niche for undifferentiated spermatogonia, germ cell tumors, and spermatid elongation. Stem Cells *28*, 1424–1434.

Ping, X.L., Sun, B.F., Wang, L., Xiao, W., Yang, X., Wang, W.J., Adhikari, S., Shi, Y., Lv, Y., Chen, Y.S., et al. (2014). Mammalian WTAP is a regulatory subunit of the RNA N^6-methyladenosine methyltransferase. Cell Res. *24*, 177–189.

Robinson, M.D., McCarthy, D.J., and Smyth, G.K. (2010). edgeR: a Bioconductor package for differential expression analysis of digital gene expression data. Bioinformatics *26*, 139–140.

Teletin, M., Vernet, N., Yu, J.S., Klopfenstein, M., Jones, J.W., Feret, B., Kane, M.A., Ghyselinck, N.B., and Mark, M. (2019). Two functionally redundant sources of retinoic acid secure spermatogonia differentiation in the seminiferous epithelium. Development *146*, dev170225.

Trapnell, C., Roberts, A., Goff, L., Pertea, G., Kim, D., Kelley, D.R., Pimentel, H., Salzberg, S.L., Rinn, J.L., and Pachter, L. (2012). Differential gene and transcript expression analysis of RNA-seq experiments with TopHat and Cufflinks. Nat. Protoc. *7*, 562–578.

Wang, T., Cui, Y.Z., Jin, J.J., Guo, J.H., Wang, G.B., Yin, X.F., He, Q.Y., and Zhang, G. (2013). Translating mRNAs strongly correlate to proteins in a multivariate manner and their translation ratios are phenotype specific. Nucleic Acids Res. *41*, 4743–4754.

Wang, X., Feng, J., Xue, Y., Guan, Z.Y., Zhang, D.L., Liu, Z., Gong, Z., Wang, Q., Huang, J.B., Tang, C., et al. (2016). Structural basis of N^6-adenosine methylation by the METTL3-METTL14 complex. Nature *534*, 575–578.

Wang, Y., Li, Y., Yue, M.H., Wang, J., Kumar, S., Wechsler-Reya, R.J., Zhang, Z.L., Ogawa, Y., Kellis, M., Duester, G., et al. (2018). N^6-methyladenosine RNA modification regulates embryonic neural stem cell self-renewal through histone modifications. Nat. Neurosci. *21*, 195–206.

Welborn, J.P., Davis, M.G., Ebers, S.D., Stodden, G.R., Hayashi, K., Cheatwood, J.L., Rao, M.K., and MacLean, J.A., 2nd. (2015). *Rhox8* ablation in the Sertoli cells using a tissue-specific RNAi approach results in impaired male fertility in mice. Biol. Reprod. *93*, 8.

Wen, J., Lv, R.T., Ma, H.H., Shen, H.J., He, C.X., Wang, J.H., Jiao, F.F., Liu, H., Yang, P.Y., Tan, L., et al. (2018). Zc3h13 regulates nuclear RNA m^6A methylation and mouse embryonic stem cell self-renewal. Mol. Cell *69*, 1028–1038.

Wojtas, M.N., Pandey, R.R., Mendel, M., Homolka, D., Sachidanandam, R., and Pillai, R.S. (2017). Regulation of m^6A transcripts by the 3′→5′ RNA helicase YTHDC2 is essential for a successful meiotic program in the mammalian germline. Mol. Cell *68*, 374–387.

Wu, R.C., Jiang, M., Beaudet, A.L., and Wu, M.Y. (2013). ARID4A and ARID4B regulate male fertility, a functional link to the AR and RB pathways. Proc. Natl. Acad. Sci. U S A *110*, 4616–4621.

Wu, R.C., Zeng, Y., Chen, Y.F., Lanz, R.B., and Wu, M.Y. (2017). Temporal-spatial establishment of initial niche for the primary spermatogonial stem cell formation is determined by an ARID4B regulatory network. Stem Cells *35*, 1554–1565.

Yang, Q.E., Kim, D., Kaucher, A., Oatley, M.J., and Oatley, J.M. (2013). CXCL12-CXCR4 signaling is required for the maintenance of mouse spermatogonial stem cells. J. Cell Sci. *126*, 1009–1020.

Yang, Y.G., Feng, Y.M., Feng, X., Liao, S.Y., Wang, X.X., Gan, H.Y., Wang, L.X., Lin, X.W., and Han, C.S. (2016). BMP4 cooperates with retinoic acid to induce the expression of differentiation markers in cultured mouse spermatogonia. Stem Cells Int. *2016*, 9536192.

Yoon, K.J., Ringeling, F.R., Vissers, C., Jacob, F., Pokrass, M., Jimenez-Cyrus, D., Su, Y.J., Kim, N.S., Zhu, Y.H., Zheng, L., et al. (2017). Temporal control of mammalian cortical neurogenesis by m^6A methylation. Cell *171*, 877–889.

Yuen, B.T.K., Bush, K.M., Barrilleaux, B.L., Cotterman, R., and Knoepfler, P.S. (2014). Histone H3.3 regulates dynamic chromatin states during spermatogenesis. Development *141*, 3483–3494.

Zhao, B.S., Roundtree, I.A., and He, C. (2017). Post-transcriptional gene regulation by mRNA modifications. Nat. Rev. Mol. Cell Biol. *18*, 31–42.

Zheng, Q.S., Wang, X.N., Wen, Q., Zhang, Y., Chen, S.R., Zhang, J., Li, X.X., Sha, R.N., Hu, Z.Y., Gao, F., et al. (2014). *Wt1* deficiency causes undifferentiated spermatogonia accumulation and meiotic progression disruption in neonatal mice. Reproduction *147*, 45–52.